



Excessive apoptosis of *Rip1*-deficient T cells leads to premature aging

Lingxia Wang¹, Xixi Zhang¹, Haiwei Zhang¹, Kaili Lu², Ming Li¹, Xiaoming Li¹, Yangjing Ou¹, Xiaoming Zhao¹, Xiaoxia Wu¹, Xuanhui Wu¹ , Jianling Liu¹, Mingyan Xing¹, Han Liu¹, Yue Zhang³, Yongchang Tan³, Fang Li⁴, Xiaoxue Deng⁵, Jiangshan Deng², Xiaojie Zhang² , Jinbao Li⁴, Yuwu Zhao², Qirong Ding¹ , Haikun Wang⁵, Xiuzhe Wang^{2,*} , Yan Luo^{3,**} , Ben Zhou^{1,***}  & Haibing Zhang^{1,****} 

Abstract

In mammals, the most remarkable T cell variations with aging are the shrinking of the naïve T cell pool and the enlargement of the memory T cell pool, which are partially caused by thymic involution. However, the mechanism underlying the relationship between T-cell changes and aging remains unclear. In this study, we find that T-cell-specific *Rip1* KO mice show similar age-related T cell changes and exhibit signs of accelerated aging-like phenotypes, including inflammation, multiple age-related diseases, and a shorter lifespan. Mechanistically, *Rip1*-deficient T cells undergo excessive apoptosis and promote chronic inflammation. Consistent with this, blocking apoptosis by co-deletion of *Fadd* in *Rip1*-deficient T cells significantly rescues lymphopenia, the imbalance between naïve and memory T cells, and aging-like phenotypes, and prolongs life span in T-cell-specific *Rip1* KO mice. These results suggest that the reduction and hyperactivation of T cells can have a significant impact on organismal health and lifespan, underscoring the importance of maintaining T cell homeostasis for healthy aging and prevention or treatment of age-related diseases.

Keywords apoptosis; inflammation; premature aging; RIP1

Subject Categories Autophagy & Cell Death; Immunology; Molecular Biology of Disease

DOI 10.15252/embr.202357925 | Received 4 August 2023 | Revised 29 October 2023 | Accepted 2 November 2023 | Published online 15 November 2023

EMBO Reports (2023) 24: e57925

Introduction

Aging is characterized by a gradual decline in the physiological and functional capacities of tissues and organs, resulting in multimorbidity and mortality (Kubben & Misteli, 2017). Aging is a major risk factor for the development of many chronic diseases, including cancer, cardiovascular disease, neurodegeneration, and infectious diseases (Cai *et al*, 2022). Research has shown that aging disrupts immune function over time, making individuals more susceptible to various diseases (Goldberg & Dixit, 2015). Accumulating evidence has shown that changes in the immune system contribute to the onset of aging and accelerate the aging process (Mogilenko *et al*, 2022). Thus, the relationship between aging and the immune system is highly complex and intricate, and much is not fully understood.

The role of the innate immune system in age-related health problems has been studied extensively (Mogilenko *et al*, 2022). Recent studies have revealed the active involvement of the adaptive immune system in such processes, focusing on T cells (Goronzy & Weyand, 2019). Exhausted T cells have been found to produce high levels of granzyme K, exacerbating inflammation, suggesting that different subsets of age-related T cells may promote tissue damage (Mogilenko *et al*, 2021). External factors such as chronic viral infections can accelerate the accumulation of age-related T cells (Covre *et al*, 2020). Additionally, T cell-specific deletion of the mitochondrial transcription factor A (TFAM) not only causes immunometabolic dysfunction that drives T cell senescence but also leads to a general decline in overall health and the emergence of multiple aging-related features (Desdin-Mico *et al*, 2020), highlighting the crucial role of T cell aging in overall deterioration.

1 CAS Key Laboratory of Nutrition, Metabolism and Food Safety, Shanghai Institute of Nutrition and Health, University of Chinese Academy of Sciences, Chinese Academy of Sciences, Shanghai, China

2 Department of Neurology, Shanghai Sixth People's Hospital Affiliated to Shanghai Jiao Tong University School of Medicine, Shanghai, China

3 Department of Anesthesiology, Ruijin Hospital, Shanghai Jiao Tong University School of Medicine, Shanghai, China

4 Department of Anesthesiology, Shanghai First People's Hospital, Shanghai Jiaotong University, Shanghai, China

5 CAS Key Laboratory of Molecular Virology and Immunology, University of Chinese Academy of Sciences, Chinese Academy of Sciences, Shanghai, China

*Corresponding author. Tel: +86 21 64369181; E-mail: xiuzhewang@hotmail.com

**Corresponding author. Tel: +86 21 64370045-666223; E-mail: ly11087@rjh.com.cn

***Corresponding author. Tel: +86 21 54920717; E-mail: benzhou@sibs.ac.cn

****Corresponding author. Tel: +86 21 54920988; E-mail: hbzhang@sibs.ac.cn

It is now well recognized that multiple age-related biological changes can lead to defective T cell responses, but the mechanisms by which these changes affect T cells are not yet clear (Goronzy & Weyand, 2019). One of the most striking features of aging is thymic involution, in which the thymus degenerates over time and reduces the replenishment of naïve T cell pools necessary for protective immunity (Palmer *et al*, 2018; Thomas *et al*, 2020; Elyahu & Monsonego, 2021; Spadaro *et al*, 2022). Impaired naïve T cell output disrupts the composition of peripheral T cells, resulting in the compensatory expansion of pre-existing T cell clones and hyperactivation. These adaptations lead to decreased TCR diversity, impaired TCR responses, and an altered distribution of T cell subsets (Zhang *et al*, 2021). Such cellular changes and clonal expansion may contribute to the loss of immune response to diverse antigens in older adults. However, the mechanism underlying the relationship between these T-cell changes and mammalian aging remains unclear.

Receptor-interacting protein kinase 1 (RIPK1 or RIP1) plays a crucial role in regulating cell survival, inflammation, apoptosis, and necroptosis (Ofengeim & Yuan, 2013). Previous research has shown that *Rip1*-deficient mice die at birth because of systemic inflammation, which can be prevented by blocking both FADD/caspase-8-dependent apoptosis and RIP3/MLKL-dependent necroptosis (Dillon *et al*, 2014; Rickard *et al*, 2014). Patients with RIP1 deficiency experience recurrent infections, early-onset inflammatory bowel disease, and progressive polyarthritis (Delphine *et al*, 2018; Li *et al*, 2018; Uchiyama *et al*, 2019). More importantly, they exhibit T-lymphopenia, which is consistent with the phenotype of mice with a T cell-specific deletion of *Rip1*, due to excessive apoptosis (Dowling *et al*, 2016). However, it is still unknown whether pronounced T-lymphopenia and hyperactivation in T-cell-specific *Rip1*-KO mice can cause aging-related diseases or premature death.

In this study, we observed that mice lacking *Rip1* in T cells (*Rip1^{fl/fl}Cd4^{Cre}* mice, called *Rip1^{TKO}* hereafter) showed signs of accelerated aging-like phenotypes along with premature death. Mechanistically, T cells with *Rip1* deficiency undergo excessive apoptosis, leading to T-lymphopenia, and increased levels of inflammation, eventually resulting in a shorter lifespan. Importantly, blocking necroptosis had little effect on the T cell compartment, multimorbidity and premature aging observed in *Rip1^{TKO}* mice. In contrast, blocking apoptosis by deleting *Fadd* in *Rip1*-deficient T cells significantly reversed T-lymphopenia, restored the balance between naïve and memory T cells, rescued aging-like phenotypes, and prolonged

the lifespan. These results suggest that the apoptosis of *Rip1*-deficient T cells plays a critical role in driving aging. Therefore, inhibiting T-cell apoptosis could be a novel approach for treating aging and age-related diseases.

Results

Disrupted peripheral T cell population homeostasis in *Rip1^{TKO}* mice resembles that in aged mice

In accordance with the dynamic changes in T cells in aged humans (Zheng *et al*, 2020; Huang *et al*, 2021; Luo *et al*, 2022), aged mice (32 months old) experienced lymphopenia with a decrease in T cells, particularly a 6% decrease in CD4⁺ T cells and a 4% decrease in CD8⁺ T cells in the spleen, compared to young mice (3 months old) (Fig 1A, and Appendix Fig S1A and B). This decrease was particularly notable for CD4⁺ and CD8⁺ naïve T cells, whereas memory T cells (CD44^{high}) were predominant in the aged group (Fig 1B and Appendix Fig S1C). Additionally, aged CD4⁺ T cells differentiated into T helper 1 (TH1) and regulatory T (Treg) subtypes as the expression of the master regulators T-bet and Foxp3 increased (Fig 1C and D, and Appendix Fig S1D and E). Furthermore, there was a significantly higher proportion of Gr1⁺CD11b⁺ cells (Fig 1E and Appendix Fig S1F) and noticeable thymic involution (Fig 1F) in aged mice. Thus, the immune system, particularly T cells, seems to play a vital role in healthy aging (Yousefzadeh *et al*, 2021; Han *et al*, 2023). Under certain circumstances, T cells contribute to age-related diseases through the secretion of proinflammatory cytokines or the release of cytotoxic granules (Carrasco *et al*, 2021), which suggests that T cell hyperactivation may accelerate the aging process and age-related diseases by promoting inflammaging, the chronic state of low-grade inflammation.

Given the key role of RIP1 in cell death and survival, a previous study reported that the T cell-specific deletion of *Rip1* in mice led to a noticeable decrease in the peripheral T cell phenotype (Dowling *et al*, 2016; Webb *et al*, 2019). This observation prompted us to investigate whether mice lacking RIP1 in T cells could simulate similar changes in T cell reduction observed in aged mice, to study the relationship between T cell changes and individual aging. To test this hypothesis, we generated mice with a conditional knockout of *Rip1* in T cells by crossing *Rip1^{fl/fl}* mice with *Cd4-Cre* transgenic mice expressing Cre recombinase under the control of the *Cd4*

Figure 1. Disrupted peripheral T cell population homeostasis in *Rip1^{TKO}* mice resembles aged mice.

- A–D Flow cytometric quantification of splenic CD4⁺ and CD8⁺ T cells (A), and T_{naïve} (CD44[−]CD62L⁺), and TCM (CD44⁺CD62L⁺), TEM (CD44⁺CD62L[−]) cells (B). Percentage of splenic CD4⁺ T cells positive for Th1 cell transcription factor T-bet (C) and Treg cell transcription factor Foxp3 (D). Mice were 3- and 32-month-old ($n = 7$ biological replicates, 3-month-old; $n = 7$ or 8 biological replicates, 32-month-old, all male, housed in the SPF condition).
- E Percentage of Gr1⁺CD11b⁺ cells in the spleen (3-month-old, $n = 7$ biological replicates, 32-month-old, $n = 8$ biological replicates).
- F Thymus weights of 3- and 32-month-old mice (3-month-old, $n = 7$ biological replicates, 32-month-old, $n = 8$ biological replicates).
- G, H Flow cytometric quantification of splenic CD4⁺ and CD8⁺ T cells (G, $n = 4–7$ biological replicates), T_{naïve}, TCM, and TEM (H, $n = 3–5$ biological replicates) of mice at different ages.
- I Percentages of Foxp3-positive cells in total mouse splenic CD4⁺ T cells at the ages indicated ($n = 3–6$ biological replicates).
- J Representative photographs showing thymic sizes of *Rip1^{fl/fl}* and *Rip1^{TKO}* mice at 6- and 12-month age (left). The graph (right) shows the thymus weight of *Rip1^{fl/fl}* and *Rip1^{TKO}* mice at 3, 6 and 12 months of age ($n = 3–6$ biological replicates).

Data information: Data are represented as mean ± SD. Dots in all graphs represent individual sample data. *P* values were calculated in (A–F) using a two-tailed unpaired Student's *t*-test, and in (G–J) using two-way ANOVA.

Source data are available online for this figure.

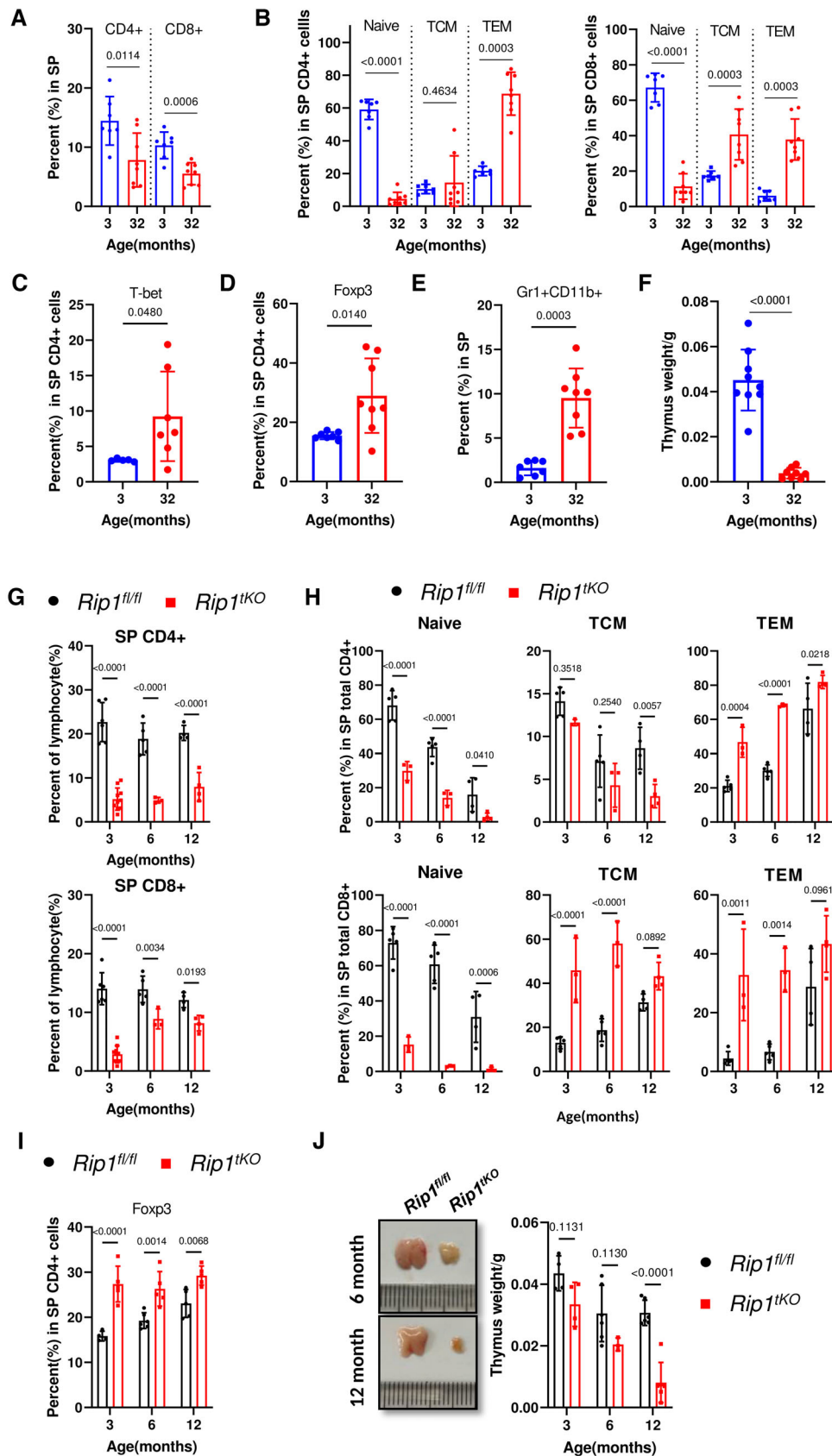


Figure 1.

promoter (Dowling *et al*, 2016). Since *Cd4-Cre* is expressed during the double-positive period in the thymus, *Rip1* was deleted in all T cells (Fig EV1A). Flow cytometric analysis revealed that *Rip1^{tko}* mice had significantly fewer mature T cells (both CD4⁺ and CD8⁺) in the spleen than age-matched control mice, regardless of age (Figs 1G and EV1B). Naïve T cells in *Rip1^{tko}* mice were notably reduced at a young age and nearly disappeared by 12 months of age, whereas the population of memory and effector T cells increased (Figs 1H and EV1C). Similar to aged WT mice, the percentage of Treg cells was higher in *Rip1^{tko}* mice spleen than in age-matched control mice (Figs 1I and EV1D). Upon further analysis at different ages, we observed severe thymic involution (Figs 1J and EV1E), which is closely associated with advanced age.

To confirm the changes in the T cell pool observed in *Rip1^{tko}* mice, we crossed *Rip1^{tko}* mice with *Rosa26^{CAG-loxp-STOP-loxp-tdTomato}* (*R26^{tdTomato}*) mice to generate T cell tracing mice (*Rip1^{tko}R26^{tdTomato}*), in which all *Cd4-Cre*-expressing cells and their descendants were constitutively labeled with tomato fluorescence. We also observed that the number of T cells dramatically decreased in solid organs, including the kidney, liver, and heart of *Rip1^{tko}R26^{tdTomato}* mice (Fig EV1F and Appendix Fig S2). These data demonstrate that RIP1 is critical for maintaining peripheral T cell homeostasis. The reduction in T cells and the overactivation state in *Rip1^{tko}* mice resemble the T cell status of aged individuals, which prompted us to further investigate whether *Rip1*-deficient T cells could accelerate the aging process.

***Rip1^{tko}* mice display aggravated premature aging phenotypes and shortened lifespan**

Consistent with a previous report (Dowling *et al*, 2016), *Rip1^{tko}* mice appeared healthy and were indistinguishable from *Rip1^{fl/fl}* mice until adulthood. However, we observed physical deterioration in *Rip1^{tko}* mice at approximately 6 months of age. Hindlimb clasp was first observed when *Rip1^{tko}* mice reached 6 months of

age and it became more severe over time, accompanied by other macroscopic changes such as hypotrichosis and graying of the fur (Fig 2A). Both male and female *Rip1^{tko}* mice exhibited lower body weights (Fig 2B and C). We observed a higher incidence of kyphosis in *Rip1^{tko}* mice (Fig 2D), which is an important indicator of aging.

To assess the overall fitness of the animals, we evaluated their voluntary movements, coordination, muscle strength, and motor function. Notably, *Rip1^{tko}* mice showed higher clasping scores, poorer performance in the rotarod test, less movement in the open field test, decreased grip strength, worse coordination in the hang-wire test, and a shortened lifespan than age-matched control mice (Figs 2E–J, and EV2A and B). Our observations suggest that *Rip1^{tko}* mice exhibit premature aging phenotypes.

To further evaluate the potential of *Rip1^{tko}* mice as age-related disorder models, we comprehensively examined their skeleton, muscle function, and lipid metabolism. We performed micro-computed tomography (micro-CT) scans of the tibia and femur of 12-month-old *Rip1^{tko}* mice and age-matched control mice. Our analysis of the three-dimensional structural data indicated that *Rip1^{tko}* mice developed osteoporosis, which was characterized by a loss of bone value in both the tibia and femur, a decrease in the number (Th.N) and thickness (Th.Th) of bone trabeculae, and an increase in the trabecular space (Th.Sp) compared to control mice (Figs 2K, and EV2C and D). Additionally, histological analyses revealed a reduction in the mean fiber area of muscle tissue in *Rip1^{tko}* mice compared to that in the control mice (Fig 2L). Another age-related pathology observed was the thinning of the epidermis. The loss of subcutaneous fat in *Rip1^{tko}* mice resulted in significantly reduced skin thickness compared to that in control mice (Fig 2M). *Rip1^{tko}* mice also had smaller adipocytes, as shown by histological analyses (Fig 2N) and loss of body fat mass, as measured by magnetic resonance imaging (MRI) (Fig EV2E). In summary, our findings suggest that *Rip1*-deficient T cells cause osteoporosis, sarcopenia and lipolysis, resulting in premature aging and the progression of age-associated disorders.

Figure 2. *Rip1^{tko}* mice develop premature aging phenotypes and age-related multi disfunctions.

- A Representative photograph of 12-month-old female *Rip1^{fl/fl}* and *Rip1^{tko}* mice.
- B Body weight evolution in male *Rip1^{fl/fl}* and *Rip1^{tko}* mice ($n = 10$ –15 biological replicates).
- C Body weight evolution in female *Rip1^{fl/fl}* and *Rip1^{tko}* mice ($n = 10$ –15 biological replicates).
- D Quantification of spine curvature by micro-computed tomography (CT) scans (left) and percentage of mice presenting lordokyphosis (right) in 12-month-old *Rip1^{fl/fl}* and *Rip1^{tko}* mice ($n = 10$ –11 biological replicates).
- E Example of hindlimb clasping phenotype in 12-month-old *Rip1^{fl/fl}* and *Rip1^{tko}* mice (left) and hindlimb clasping score (right; $n = 10$ –19 biological replicates) in 20-s test at the indicated age. Boxplots depict the median and interquartile range, with whiskers extending to the maximum and minimum of the data. + denotes the mean.
- F Rotarod performance of 12-month-old *Rip1^{fl/fl}* and *Rip1^{tko}* mice, expressed as the average time spent on the rotating rod in four combined trials ($n = 4$ –5 biological replicates).
- G–I Total travel distance in the open field test (G), grip strength (H), and hanging endurance (I) of 12-month-old *Rip1^{fl/fl}* and *Rip1^{tko}* mice ($n = 4$ –9 biological replicates).
- J Kaplan–Meier survival curves for *Rip1^{fl/fl}* and *Rip1^{tko}* mice ($n = 17$ –23 biological replicates, including males and females).
- K Representative micro-CT 3D reconstructed images (left; scale bar, 1 mm) and quantification of the femur trabecular bone volume fraction (BV/TV) (right) in 12-month-old male *Rip1^{fl/fl}* and *Rip1^{tko}* mice ($n = 6$ –8 biological replicates).
- L Representative hematoxylin and eosin (H&E)-stained sections of the tibia anterior muscle (left; scale bar, 100 μ m) and quantification of mean myofiber cross-sectional area (right; $n = 5$ –6 biological replicates; 10-month-old mice).
- M Representative skin sections stained with Masson's trichrome (left; scale bar, 100 μ m) and quantification of hypodermal fat thickness (right). Graph shows the mean values of five mice at 12 months of age.
- N Representative H&E-stained sections of gWAT (left; scale bar, 100 μ m) and quantification of mean estimated adipocyte surface area (right; $n = 4$ biological replicates).

Data information: Data are represented as mean \pm SD. Dots in all graphs represent individual sample data. *P* values were calculated in (F), (G–I), and (K–N) using a two-tailed unpaired Student's *t*-test, in (B), (C), and (E) using two-way ANOVA, in (J) using the log-rank test.

Source data are available online for this figure.

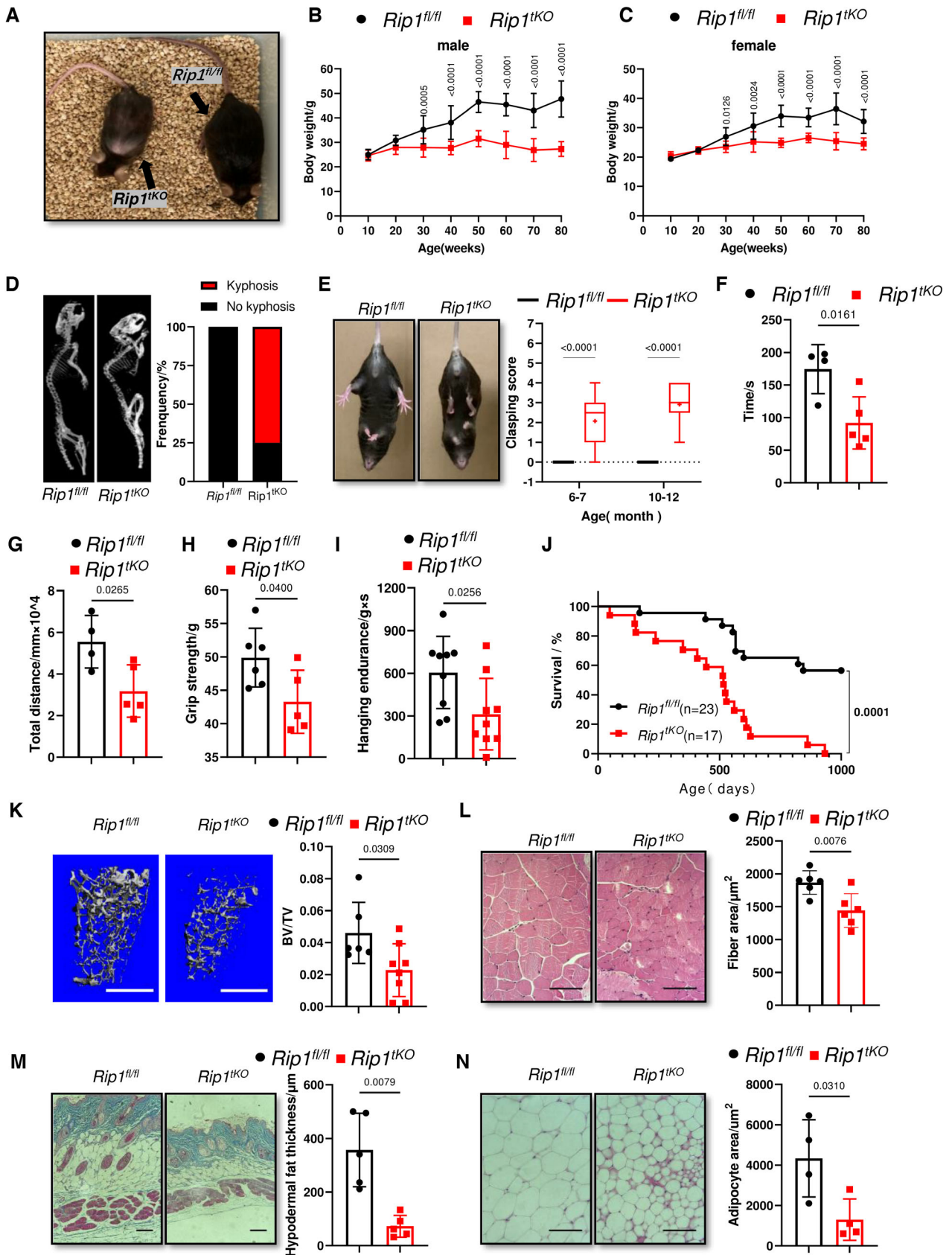


Figure 2.

Rip1^{tko} mice exhibit enhanced inflammation and senescence markers

Age-related disorders are characterized by chronic and progressive low-grade inflammation (Bernal *et al*, 2014; Jurk *et al*, 2014; Lopez-Otin *et al*, 2022). To investigate the mechanisms underlying multi-morbidity and frailty in Rip1^{tko} mice, we performed primary T-cell transcriptomics. The results of gene-ontology (GO) analysis showed that the upregulated differentially expressed genes in Rip1-deficient T cells were mainly enriched in inflammation and immune cell activation, such as activation of myeloid leukocytes and the interleukin-18 signaling pathway (Fig EV3A). Additionally, Rip1-deficient T cells exhibited inflammatory, cytotoxic, and activation-related transcriptomic features, including elevated expression levels of *Ilr1*, *Il1b*, *Gzmb*, and *Klrg1* (Fig EV3B). We also observed higher levels of circulating chemokines and cytokines (Fig 3A), and an increased proportion of Gr1⁺CD11b⁺ cells in the spleens (Fig 3B) of 12-month-old Rip1^{tko} mice than in age-matched control mice, indicating the presence of circulating inflammation. The Rip1^{tko} mice showed comparable serum antinuclear antibodies (ANAs) (Fig EV3C). Additionally, Rip1-deficient T cells secreted higher levels of the inflammatory cytokines IL-17A and interferon- γ (IFN- γ) as well as the transcription factors T-bet and ROR γ t (Fig 3C and D, and Appendix Fig S3A and B) in CD4⁺ subset and higher IFN- γ in CD8⁺ T cells (Fig 3E and Appendix Fig S3A). These results demonstrate that Rip1-deficient T cells lead to inflammation through vigorous inflammatory cytokine production.

Given that T cells may induce senescence through pro-inflammatory cytokines (Braumuller *et al*, 2013; Carrasco *et al*, 2021), we tested whether plasma pro-inflammatory cytokines in Rip1^{tko} mice could directly induce cellular senescence. We cultured non-senescent primary mouse dermal fibroblasts (MDFs) using medium mixed with 5% mouse plasma from 12-month-old mice. Compared with plasma from age-matched control mice, plasma from Rip1^{tko} mice stimulated MDFs showed increased expression of the senescence marker P53 and P21^{Waf/Cip1} (Fig 3F). Additionally, Rip1^{tko} mice showed elevated protein levels of senescence markers in the hearts, lungs, kidneys, livers, gonadal white adipose tissue (GAT), and intestines (Figs 3G and EV3D). We also detected an increase in senescence-associated β -galactosidase activity, a common biomarker for senescent cells in tissues and in culture (Dimri *et al*, 1995), in the kidney, lung, and liver of Rip1^{tko} mice (Fig EV3E). These results suggested that Rip1-

deficient T cells drive systemic senescence by promoting chronic inflammation.

FADD-mediated apoptosis plays a crucial role in maintaining T cell homeostasis in Rip1^{tko} mice

Since RIP1 serves as a key upstream regulator of necroptosis, apoptosis, and inflammation, and its death pattern is cell type-specific (Dannappel *et al*, 2014; Roderick *et al*, 2014; Lin *et al*, 2016; Newton *et al*, 2016; O'Donnell *et al*, 2018; Xu *et al*, 2018), we aimed to uncover the downstream effectors responsible for the observed lymphopenia and T cell hyperactivation in Rip1^{tko} mice. Given that RIP1 blocks both FADD/caspase-8-dependent apoptosis and RIP3/MLKL-dependent necroptosis during development (Dillon *et al*, 2014; Rickard *et al*, 2014), we crossed Rip1^{tko} mice with Rip3^{-/-} (He *et al*, 2009), *Mkl1*^{-/-} (Sun *et al*, 2012), and *Fadd*^{-/-}*Fadd:GFP*⁺ (Chinnaiyan *et al*, 1995; Zhang *et al*, 2005) mice. The results showed that the absence of either Rip3 or *Mkl1* had no impact on the reduced ratio or heightened T cell activation in the spleen of Rip1^{tko} mice (Fig EV4A and B). Furthermore, hind limb claspings, thinning of the back skin (Fig EV4C), and shortened lifespan (Fig EV4D) remained unchanged in these mice, indicating that necroptosis is not involved in RIP1-regulated T cell homeostasis or age-related disorders in Rip1^{tko} mice.

In contrast, eight-week-old Rip1^{fl/fl}*Fadd*^{-/-}*Fadd:GFP*⁺*Cd4*^{Cre} mice (hereafter referred to as Rip1^{tko}*Fadd*^{tko}) showed a significantly recovered percentage of T cells in the spleen compared to Rip1^{tko} mice (Figs EV4A and EV5A), indicating the dominant role of apoptosis in T cell homeostasis. Additionally, we conducted T cell transcriptomics and observed that T cells sorted from Rip1^{tko} mice showed significantly upregulated genes associated with apoptosis (Fig 4A), confirmed by western blot analysis, which revealed an increase in cleaved caspase-3 expression levels in both CD4⁺ and CD8⁺ T cells from Rip1^{tko} mice compared to those in control mice (Fig 4B). The proportions of CD4⁺ and CD8⁺ T cells in the spleen were significantly restored in Rip1^{tko}*Fadd*^{tko} mice of different ages (Fig 4C). Importantly, in Rip1^{tko}*Fadd*^{tko} mice, the naïve T cell pool was nearly completely recovered, and the memory population shrank to a level comparable to that in control mice (Fig 4D). Furthermore, fewer Gr1⁺CD11b⁺ cells, Th1/Th17 T cell skewing, and Treg cell percentages were observed in the spleens of Rip1^{tko}*Fadd*^{tko} mice (Figs 4E–G and EV5B) compared to those in Rip1^{tko} mice, implying alleviated inflammation in Rip1^{tko}*Fadd*^{tko}

Figure 3. Rip1^{tko} mice exhibit enhanced inflammation and senescence markers.

- A Serum levels of inflammatory cytokines and chemokines detected using a multiplex assay in 12-month-old Rip1^{fl/fl} and Rip1^{tko} mice ($n = 6$ biological replicates).
 B Percentage of Gr1⁺CD11b⁺ cells in the spleen of Rip1^{fl/fl} and Rip1^{tko} mice at the indicated ages ($n = 4–5$ biological replicates).
 C–E Flow cytometric quantification of splenic CD4⁺ T cells staining positive for intracellular IL-17A and IFN γ (C), Th1 cell transcription factor T-bet, Th17 cell transcription factor ROR γ t, and Th2 cell transcription factor GATA3 (D), CD8⁺ IFN- γ ⁺ T cells (E) ($n = 5–9$ biological replicates).
 F Representative immunoblot (left) and densitometric analysis (right; $n = 7–9$ biological replicates) of P53 and P21 expression in primary WT mouse dermal fibroblasts (MDFs) cultured for 3 and 7 days in the presence of 12-month-old Rip1^{fl/fl} or Rip1^{tko} mice serum. GAPDH was used as a loading control. Each lane represents the serum of independent mice used in the experiment.
 G Representative immunoblot and quantification of P53, P21, and P16 protein expression in the lung ($n = 6–8$ biological replicates), kidney ($n = 8$ biological replicates), and liver ($n = 8$ biological replicates) from 12-month-old Rip1^{fl/fl} and Rip1^{tko} mice. Loading controls were β -actin and GAPDH. The dots in all panels represent individual sample data.

Data information: Data are represented as mean \pm SD. Dots in all graphs represent individual sample data. P values were calculated in (A) and (C–G) using a two-tailed unpaired Student's t -test, and in (B) using two-way ANOVA.

Source data are available online for this figure.

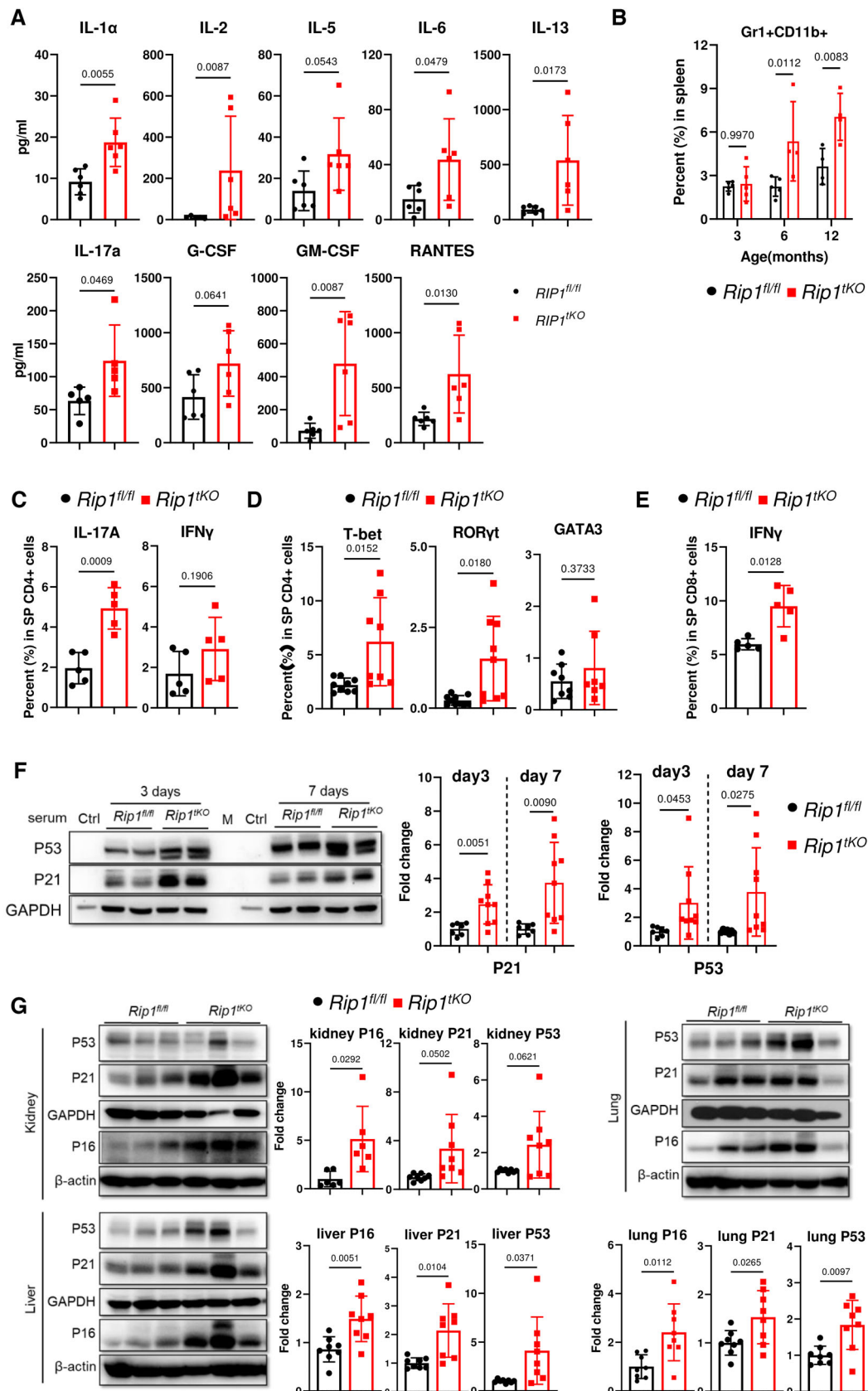


Figure 3.

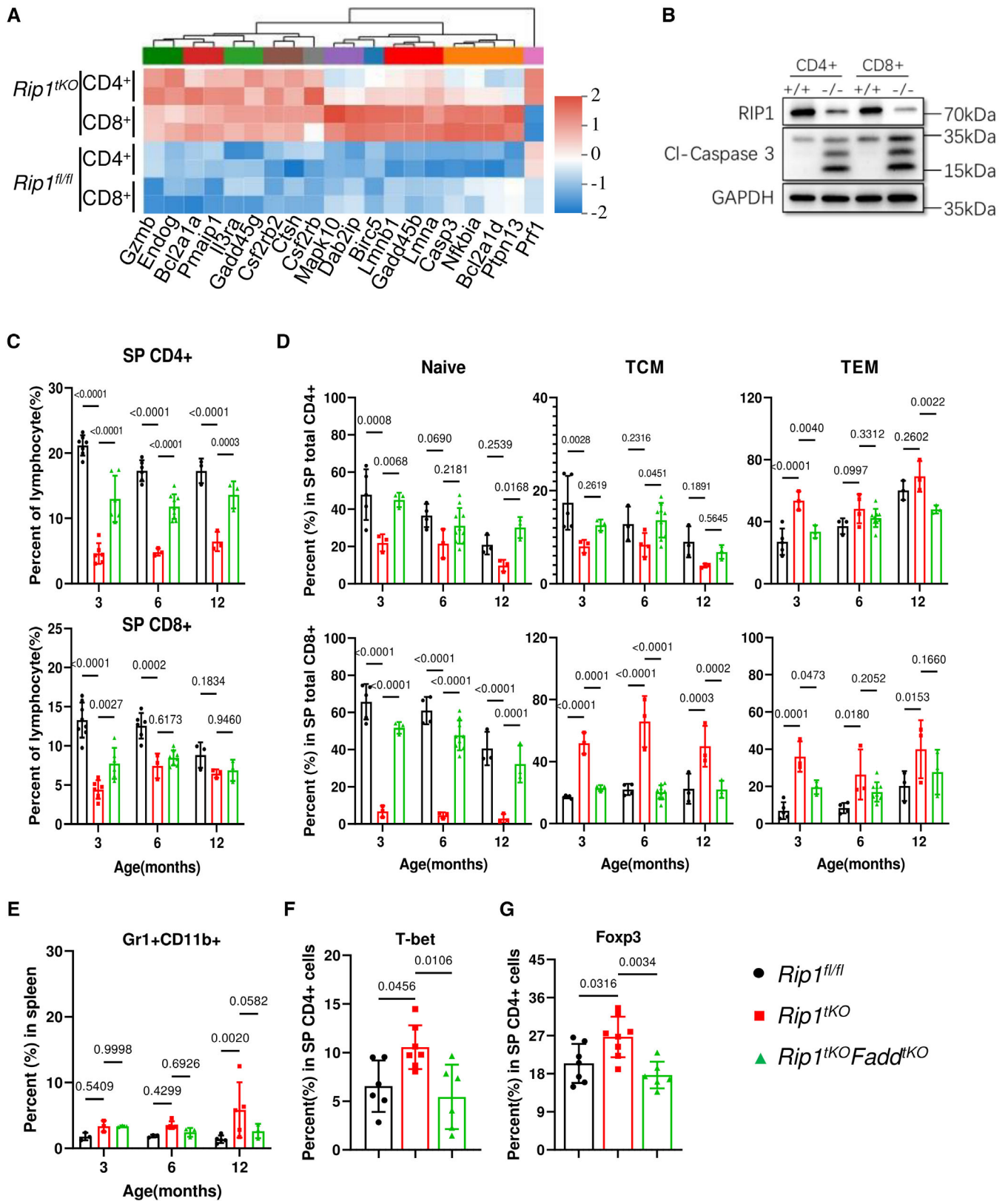


Figure 4.

Figure 4. Blocking apoptosis in great part rescues peripheral T cell homeostasis in *Rip1*^{tko} mice.

- A Heatmap depicting the apoptosis-related genes upregulated in *Rip1*-deficient CD4⁺ and CD8⁺ T cells ($n = 2$ biological replicates).
 B Representative immunoblot of apoptosis marker in CD4⁺ and CD8⁺ T cells sorted from 2-month-old mice (+/+ represents T cells isolated from *Rip1*^{fl/fl} mice and -/- from *Rip1*^{tko}. Cl-caspase-3: cleaved-caspase-3).
 C, D Flow cytometry quantification of splenic CD4⁺ and CD8⁺ T cells (C, $n = 3-7$ biological replicates), T_{naive}, TCM, and TEM (D, $n = 3-7$ biological replicates) of *Rip1*^{fl/fl}, *Rip1*^{tko}, and *Rip1*^{tko}*Fadd*^{tko} mice at the indicated age.
 E Percentage of Gr1⁺CD11b⁺ cells in the spleen of mice at the indicated age ($n = 3-5$ biological replicates).
 F, G Percentage of splenic CD4⁺ T cells positive for T-bet (F) and Foxp3 (G) ($n = 6-8$ biological replicates).

Data information: Data are represented as mean \pm SD. Dots in all graphs represent individual sample data. *P* values were calculated in (C–E) using two-way ANOVA, and in (F, G) using one-way ANOVA.

Source data are available online for this figure.

mice. These results suggest that *Rip1*-deficient T cells died in an autonomous manner of apoptosis, which formed feedback loops, leading to T cell overactivation, which was restored by *Fadd* deletion in T cells. Thus, maintaining T-cell homeostasis may be a critical element sustaining healthy physical conditions.

Blocking T cell apoptosis rescues premature aging and multimorbidity in *Rip1*^{tko} mice

Next, we examined the impact of deficiency of *Fadd* in T cells on premature aging and multimorbidity in *Rip1*^{tko} mice. Our results showed that *Rip1*^{tko}*Fadd*^{tko} mice had a longer lifespan (Fig 5A) with normal body weight gain (Fig EV5C) and ameliorated thymic involution (Fig 5B) than *Rip1*^{tko} mice. Additionally, age-related disorders such as hindlimb claspings (Fig 5C), sarcopenia (Fig 5D), skin thinning (Fig 5E), osteoporosis (Figs 5F, and EV5D and E), and excessive lipolysis (Fig 5G), which were present in *Rip1*^{tko} mice, were fully prevented in *Rip1*^{tko}*Fadd*^{tko} mice. Furthermore, blocking FADD-mediated apoptosis in T cells improved the physical quality of *Rip1*^{tko} mice, as assessed by hanging endurance (Fig 5H), rotarod performance (Figs 5I and EV5F), and movement in an open field test (Fig EV5G). Finally, blocking T-cell apoptosis prevented multiple instances of tissue senescence in *Rip1*^{tko} mice (Figs 5J, and EV5H and I). These findings suggest that maintaining T cell homeostasis by blocking apoptosis in *Rip1*^{tko} mice can prevent premature aging and multimorbidity syndromes.

Discussion

In this report, we demonstrate that T-cell-specific *Rip1* deficiency mice experience age-related multimorbidity, including hair loss, hindlimb claspings, kyphosis, reduced motor coordination, osteoporosis, sarcopenia, abnormal fat metabolism, and ultimately premature death. Blocking necroptosis by crossing *Rip3*^{-/-} or *Mkl1*^{-/-} with *Rip1*^{tko} mice had no effect on the aging phenotypes, whereas blocking apoptosis by deleting *Fadd* in T cells restored the balance between naïve and memory T cells and rescued aging-related phenotypes, ultimately extending the lifespan of *Rip1*^{tko} mice. Our results suggest that T-cell apoptosis is a driving factor in the aging process, and we propose that inhibiting T-cell apoptosis has the potential to offer new therapies for aging and age-related diseases.

In recent years, there has been an explosion of research exploring the mechanisms underlying aging. In this study, we showed that T cell pool shrinkage and overactivation can induce premature aging and age-related multimorbidity, which is mediated by inflammation in *Rip1*^{tko} mice. Moreover, *Rip1*-deficient T cells had a higher proportion of cells undergoing the cell cycle and acquiring a highly differentiated and cytotoxic phenotype (Fig EV3B). Consistent with this, HIV-infected patients suffer owing to the death of CD4⁺ T cells (Doitsh et al, 2014) and subsequent chronic diseases, which resemble some aspects of immune senescence and premature aging (Gross et al, 2016; Esteban-Cantos et al, 2021; Breen et al, 2022). Our findings emphasize the crucial role of maintaining a normal T cell balance in preventing premature aging and provide a potential

Figure 5. *Rip1*^{tko}*Fadd*^{tko} mice show lower rates of age-related disorders and counteract accelerated aging process.

- A Kaplan–Meier survival curves for *Rip1*^{tko} and *Rip1*^{tko}*Fadd*^{tko} mice ($n = 22-29$ biological replicates, including males and females).
 B Thymus photograph of *Rip1*^{fl/fl}, *Rip1*^{tko}, and *Rip1*^{tko}*Fadd*^{tko} mice at the age of 12-month (left) and weights at 3, 6, and 12 months of age ($n = 3-7$ biological replicates).
 C Hindlimb claspings phenotype in 12-month-old mice (left) and hindlimb claspings scores (right; $n = 10-29$ biological replicates) in 20-s test at the indicated age. Boxplots depict the median and interquartile range, with whiskers extending to the maximum and minimum of the data. + denotes the mean.
 D Representative images of H&E-stained tibia anterior muscle from 12-month-old mice (left; scale bar, 100 μ m) and quantification of mean myofiber cross-sectional area (right; $n = 3-6$ biological replicates).
 E Representative H&E-stained skin sections (left; scale bar, 100 μ m) and quantification of hypodermal fat thickness (right) ($n = 3$ biological replicates; 12-month-old mice).
 F Representative micro-CT 3D reconstructed images (left; scale bar, 1 mm) and quantification of the femur trabecular index BV/TV (right) in 12-month-old males ($n = 5-6$ biological replicates).
 G Percentage of adipose tissue determined by quantitative magnetic resonance imaging in mice at 30 and 50-week-old age ($n = 6-8$ biological replicates).
 H Hanging endurance of 12-month-old female mice ($n = 7-10$ biological replicates).
 I Rotarod performance by 12-month-old mice ($n = 6-10$ biological replicates).
 J Immunoblot of P53, P21, and P16 protein expression in the kidney, lungs, and liver of 12-month-old mice. Each lane represents individual sample data.

Data information: Data are represented as mean \pm SD. Dots in all graphs represent individual sample data. *P* values were calculated in (A) using the log-rank test, in (C) and (G) using two-way ANOVA, and in (D–F) and (H, I) using one-way ANOVA.

Source data are available online for this figure.

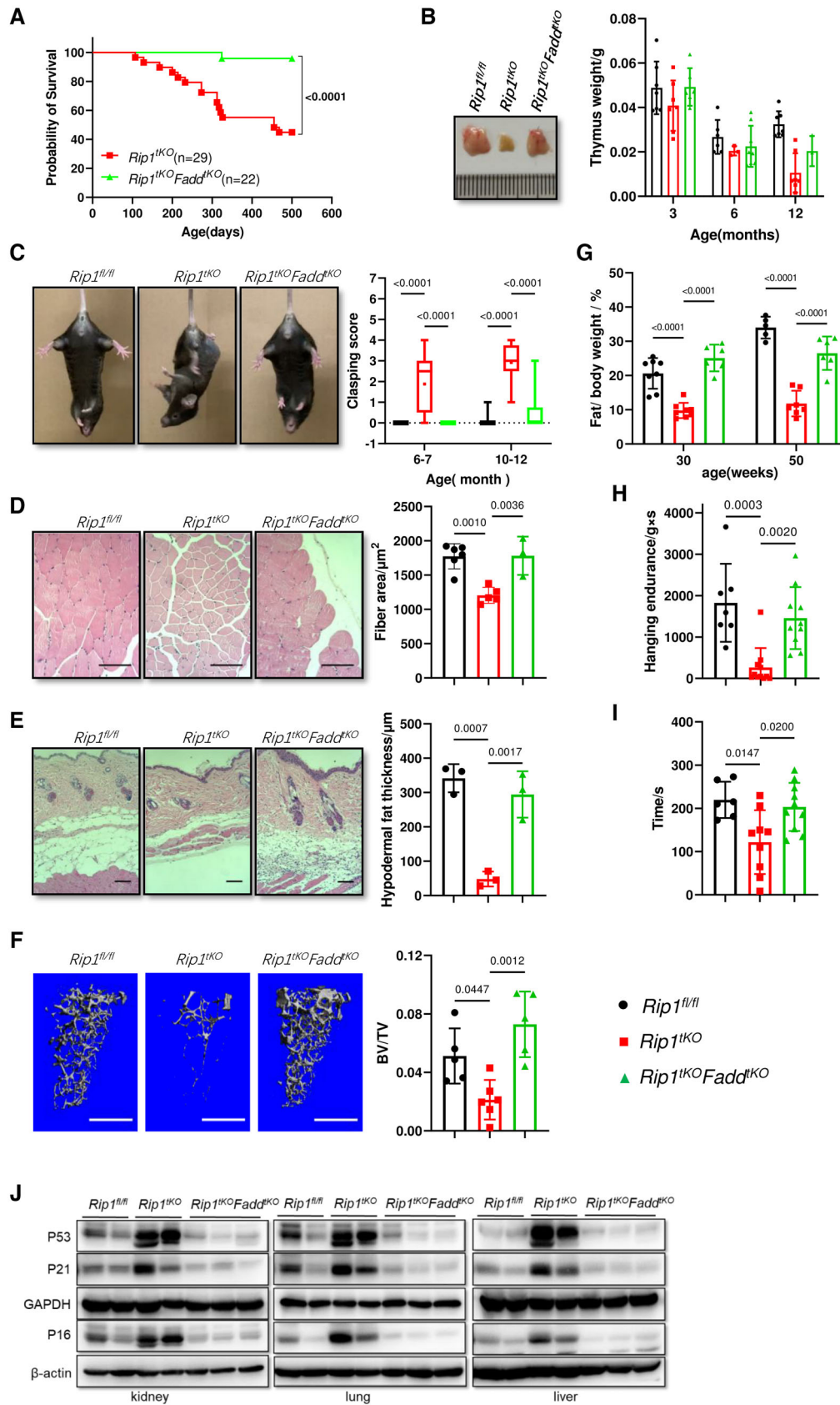


Figure 5.

explanation for the many premature aging phenotypes observed in diseases such as AIDS, which are characterized by a decrease in T lymphocytes.

A previous study (Gupta *et al*, 2018) and our data, as shown in Appendix Fig S4A and B, indicate that the expression of RIP1 in T cells is significantly lower in aged individuals than in young individuals, whereas RIP1 downstream molecules associated with apoptosis, cleaved caspase-3 for instance, are increased. T-cells are constantly exposed to diverse antigens and undergo continuous cycles of clonal expansion, death, and memory subtypes survival (Goronzy & Weyand, 2019). However, the exact roles of RIP1-regulated pathways in these processes remain unclear. We hypothesized that RIP1 plays a pro-survival role at certain stages of the T cell journey, while cell death serves as a checkpoint to control clonal expansion and to terminate uncontrolled responses. This may explain why the loss of RIP1 expression in T cells contributes to accelerated aging. Additionally, IL-7/IL-7R signaling is crucial for the homeostatic proliferation and survival of naïve T cells (Maraskovsky *et al*, 1996; Tan *et al*, 2001), and the expression of IL-7R is impaired in peripheral T cells in *Rip1^{tko}* mice (Webb *et al*, 2019). Whether IL-7R expression would be restored in *Rip1^{tko}Fadd^{tko}* mice remains exclusive. We thus measured IL-7R in *Rip1^{tko}Fadd^{tko}* mice. Our data showed that IL-7R expression was partially restored in CD4⁺ T cells of *Rip1^{tko}Fadd^{tko}* mice but not CD8⁺ T cells compared to *Rip1^{tko}* mice (Appendix Fig S5A). These findings further support the hypothesis that RIP1 expression is necessary for the survival of peripheral T cells. Therefore, it is necessary to clarify the dynamic nature of RIP1 in T cells during aging, which will help guide the maintenance of individual health by regulating T cell survival.

Deletion of *Fadd* has a significant effect on the restoration of the T cell compartment in *Rip1^{tko}* mice. Interestingly, *Rip1^{tko}Fadd^{tko}* double knock-out mice appeared healthier than control mice, suggesting that there may be a minimum number of T cells required to maintain physiological and functional fitness. Our experiments revealed that RIP3/MLKL-mediated pathways are not involved in *Rip1* knock-out T cells, demonstrating that the primary function of RIP1 in T cells is to protect against apoptosis. However, the specific molecular triggers that activate this cell death pathway remain unknown. Deletion of *Rip1* substantially increases the sensitivity of thymocytes to TNF-induced death (Dowling *et al*, 2016), so we crossed *Tnfr1* knock-out mice with *Rip1^{tko}* mice to test whether disrupting TNFR1-mediated signaling could rescue the peripheral T-cell defect. However, our results showed that TNFR1-KO had little recovery effect on T cell quantity (Appendix Fig S6A), suggesting that either the TNFR2 pathway was still active or that signaling molecules other than TNFRs were involved.

Our study revealed that *Rip1^{tko}* mice exhibit signs of accelerated aging and premature death. By deleting the *Fadd* gene in *Rip1*-deficient T cells, we observed the rescue of aging-related phenotypes and an extended lifespan. In a parallel investigation, Imanishi *et al* (2023) found that *Rip1* knock-out CD4⁺ T cells showed higher activation levels of Akt, mTORC1, and ERK, leading to T cell senescence, and these phenotypes of T cell senescence can be restored by a combined deficiency of *Rip3* and *Caspase-8*. These researchers concluded that the absence of *Rip1* triggers the activation of RIP3/caspase-8 and mTORC1, contributing to T cell senescence, age-related diseases, and premature death (Imanishi *et al*, 2023). However, our genetic results showed that blocking necroptosis by

deleting *Rip3* or *Mkl1* did not improve premature aging or the multiple diseases observed in *Rip1^{tko}* mice. In contrast, blocking apoptosis through deletion of *Fadd* in T cells was sufficient to completely rescue aging-related phenotypes and shortened lifespan of *Rip1^{tko}* mice. Owing to the pronounced distinctions at the cellular level that are not directly equivalent to the individual level, a more comprehensive assessment of the discrepancies between the two studies and the potential reasons would help guide the field. Further studies should involve the construction and simultaneous analysis of various genotypes in mouse models, including *RIP1^{tko}*, *Rip1^{tko}Caspase8^{tko}*, *Rip1^{tko}Rip3^{tko}*, and *Rip1^{tko}Caspase8^{tko}Rip3^{tko}*. Analysis of both cellular and individual aging phenotypes, along with the underlying mechanisms at both the cellular and organismal levels, is needed. This approach could elucidate why *Rip1* deficiency promotes T cell aging and individual aging, unraveling the mechanistic roles of different death pathways in T cell aging.

The mechanisms underlying the decline in T cells with aging and their impacts on various organs are not yet fully understood. T cells are essential for the immune system as they protect the body against pathogens and malignant cells. However, as the body ages, the quantity and effectiveness of T cells decrease, resulting in a weakened immune response and increased susceptibility to infections and diseases (Han *et al*, 2023). Moreover, studies have indicated that T cells play a role in regulating oxidative stress, a process by which harmful byproducts of cellular metabolism can damage cells and tissues (Carrasco *et al*, 2021). However, the exact mechanisms underlying how T cell aging-related changes trigger aging in various organs and eventually lead to individual death remain unclear. To gain a better understanding of the complex interactions between T cells and aging in different organs, the *Rip1^{tko}* mouse model, which is induced by a specific factor that causes T cell decline, can be used as a valuable tool.

Our findings have established that the decline of T cells in *Rip1^{tko}* mice, resembling that of aged wild-type mice, is one of the reasons for organ and individual aging and premature death. Restoration of the decrease in T cells can restore organ and individual aging in *Rip1^{tko}* mice. These results suggest that it may be clinically possible to delay aging or treat age-related diseases by blocking excessive apoptosis of T cells or by externally supplementing T cells.

Materials and Methods

Mice

All mice used in this project were maintained in a specific pathogen-free (SPF) facility. *Rip1^{fl/fl}* mice were generated by homologous recombination strategy (Shanghai Model Organisms Center, Inc.). In brief, hybrid mouse ES cells were electroporated with a targeting vector containing floxed exon 3. The ES cells were selected by G418 and ganciclovir and screened for homologous recombination by PCR. Positive clones were then injected into C57BL/6 blastocysts, which were implanted into the uterus of pseudopregnant females to generate chimeras. These chimeras were then backcrossed with C57BL/6J mice for at least 10 generations to generate *Rip1^{fl/fl}* mice. *Cd4-Cre* transgene mice were kindly provided by Professor Zichun Hua (Nanjing University). *Rosa26^{CAG-loxp-STOP-loxp-tdTomato}* mice were

obtained from Shanghai Model Organisms Center, Inc. *Rip3*^{-/-}, *Mkl1*^{-/-} and *Fadd*^{-/-}*Fadd:GFP*⁺ and *Tnfr1*^{-/-} mice lines have been previously described (Fan et al, 2016; Zhang et al, 2016, 2019). All animal experiments were conducted in accordance with the guidelines of the Institutional Animal Care and Use Committee of the Institute of Nutrition and Health, Shanghai Institutes for Biological Sciences, University of Chinese Academy of Sciences.

Reagents and antibodies

Antibodies used for western blotting listed as following: RIP1 (Cell Signaling Technology, 3493P), Cleaved caspase-3 (Cell Signaling Technology, 9661), FADD (Abcam, 124812), P53 (Cell Signaling Technology, 2524T), P21^{Waf1/Cip1} (BD Biosciences, 556431), P16^{INK4a} (Abcam, 211542), GAPDH (Sigma, G9545), β -actin (Sigma, A3854), Caspase-8 (ENZO, ALX-804-447-C100), RIP3 (ProSci, 2283).

Flow cytometry

Flow cytometric analysis was performed on Beckman CytoFlex S and data were analyzed with CytoExpert. After obtaining single cell suspensions, red blood cells were removed by incubation with a lysis buffer. For intracellular staining, Foxp3/Transcription Factor Staining Buffer Set (eBioscience, 00-5523-00) was used. For cytokine analysis, T cells were stimulated with PMA (Sigma, P1585) and ionomycin (Sigma, I3909) for 4 h followed brefeldin A stimulation for another 2 h. All the samples in the same experiments and comparisons were gated under the same parameters.

Sorting of T cells were performed on the Beckman MoFlo Astrios sorter. Mouse total primary T cells were isolated from the spleen and peripheral lymph nodes of mice by EasySep Mouse T Cell Isolation (Stemcell, 19851) and then were further sorted by flow cytometric cell sorting based on CD3⁺CD4⁺ and CD3⁺CD8⁺ surface markers. The purified cells were used according to experimental design.

The following antibodies were used: against mouse CD45 (BD, 553080), CD3e (eBioscience, 25-0031-82; BD, 553061), CD4 (eBioscience, 47-0042-82), CD8e (Biolegend, 100732 and 100738), B220 (eBioscience, 17-0452-83), Gr-1 (eBioscience, 12-5931-83), CD11b (eBioscience, 17-0112-83), CD62L (eBioscience, 25-0621-81), CD44 (eBioscience, 17-0441-81), T-bet (Invitrogen, 25-5825-80), ROR γ t (Invitrogen, 12-6988-80), GATA3 (Biolegend, 653805), Foxp3 (eBioscience, 17-0441-81), IFN γ (Biolegend, 505825), IL-17A (Biolegend, 506919), LIVE/DEAD (Biolegend, 423101), IL-7R (BD, 560733).

Western blot

Cell pellet or tissue were lysed in RIPA lysis buffer containing 1 \times proteinase inhibitor cocktail (Roche, 5056489001), 2 mM PMSF and 1 mM DTT. After centrifugation, the protein concentration in the collected supernatants was determined using a BCA protein assay kit (Thermo Scientific, 23225). The normalized lysates were subsequently denatured in reducing 5 \times SDS loading sample buffer at 100°C for 5 min.

Micro-CT scanning and magnetic resonance imaging (MRI)

Micro-CT scanning was used for kyphosis and osteoporosis determination. Angles below 15% of the average controls were classified as

kyphosis (Desdin-Mico et al, 2020). Mice were deeply sedated using isoflurane (RWD, R510-22-8) during image acquisition. Regions of interest (ROI) were drawn for tibia and femur. Body fat content measurement was assessed by MRI (EchoMRI).

Hindlimb clasping score

For this test, mice were suspended gently by the tail and videotaped for 10–15 s. Three separate trials were taken for each mouse. Hindlimb clasping severity was rated from 0 to 4:

- 0 = hindlimbs splayed outward and away from the abdomen,
- 1 = one hindlimb retracted inwards towards the abdomen intermittently,
- 2 = both hindlimbs partially retracted inwards towards the abdomen intermittently,
- 3 = both hindlimbs continuously retracted inwards towards the abdomen,
- 4 = one or both hindlimbs continuously retracted inwards towards the abdomen plus foot weakness while walking across a wire cage top.

Scores of 0.5 were utilized when appropriate.

Physical function assessments

For hanging test, mice were placed onto the metal cage top, which was then inverted and suspended above the home cage, the latency to when the animal falls is recorded. Practice was performed before official test for 3 days. This test is performed 3 days per week with three trials per session. The average performance for each session is presented as the average of the three trials.

For open field test, mice were placed in the box for 20 min and total travel distance, the time, and track in center zone or edge zone were recorded using Cleversys software.

For rotarod test, mice were trained on the rotarod first. On the test day, mice were placed onto the rotarod, which was started at 4 r/m and accelerated from 4 to 40 r/m during a 5-min test. The latency to when the animal falls from rotarod is recorded. Results averaged from four trails over a 30-min interval.

For grip strength (g) test, a Grip Strength Meter (Columbus Instruments) was used, with results averaged over 15 trials. To measure grip strength, the mouse is swung gently by the tail so that its forelimbs contact the bar. The mouse instinctively grips the bar and is pulled horizontally backwards, exerting tension. When the tension becomes too great, the mouse releases the bar.

SA- β -galactosidase assay

SA- β -gal staining was performed using kits from Beyotime (C0602) and Cell Signaling Technology (9860S), according to the manufacturer's instructions. Briefly, OCT-embedded tissue sections on glass coverslips were washed in PBS, fixed and washed, then incubated with SA- β -Gal staining solution overnight at 37°C following the manufacturer's instructions. After completion of SA- β -Gal staining, sections were stained with nuclear fast red (Servicebio, G1035) for 5–10 min at room temperature, rinsed under running water for 1 min. Sections were dehydrated in increasing concentrations of alcohol (70–80–95–100–100%) and cleared in xylene twice. After drying, samples were examined under a bright-field microscope.

MDF culture

Primary mouse dermal fibroblasts (MDFs) were separated from the skin of newborn mice. For senescence induction by mouse serum, MDFs were cultured in Opti-MEM medium (Gibco, 31985070) with 5% serum from 12-month-old *Rip1^{fl/fl}* and *Rip1^{tkO}* mice, 1% penicillin, and 100 µg/ml streptomycin for 3 or 7 days, then cell lysis was collected for further analysis.

ELISA and Luminex detection of proinflammatory cytokines and chemokines

Serum cytokines and chemokines were detected with Bio-Plex Pro Mouse Cytokine Grp I Panel 23-plex (#M60009RDPD) using the Bio-Plex 200 system (Luminex Corporation, Austin, TX, USA). TNF-α (eBioscience, 88-7324-88), IL-1β (eBioscience, 88-7013-88), IL-6 (eBioscience, 88-7064-88), IFN-β (Biolegend, 439407) and ELISA kits were used as well.

RNASeq

Total RNA was extracted from CD4 and CD8 T cells sorted from 8-week-old mice and was measured using the NanoDrop2000 (Thermo Fisher Scientific), agarose gel electrophoresis, and Agilent2100. RNA samples displaying a 260/280 ratio of around 2.0 were used. The cDNA libraries were constructed and sequenced by Majorbio Biotech. In brief, 1 µg RNA for each sample was used for cDNA libraries construction by Illumina Truseq™ RNA sample prep Kit. The constructed DNA was enriched by PCR amplification for 15 cycles and then purified by 2% gel electrophoresis. Clone clusters were generated on the Illumina cBot and high-throughput sequencing was performed on Illumina Novaseq 6000 sequencer using NovaSeq Reagent Kits v1.5 and 2 × 150 bp paired-end reads were generated. The data were analyzed on the online tool of Majorbio Cloud Platform (<https://cloud.majorbio.com/page/tools/>).

Statistical analysis

Image-Pro Plus 6 and ImageJ were used in image and immunoblot quantification. Data in figures are presented as mean ± SD, and statistical *P* value was determined by unpaired two tailed Student's *t*-test (comparing two groups), one-way ANOVA or two-way ANOVA (comparing more than two groups), the log-rank test with GraphPad Prism 9 primed.

Data availability

RNA-seq raw data have been deposited to NCBI Sequence Read Archive (SRA) as PRJNA942498: <https://www.ncbi.nlm.nih.gov/sra/?term=PRJNA942498>.

Expanded View for this article is available [online](#).

Acknowledgements

We would like to thank Dr. Xiaodong Wang (National Institute of Biological Sciences, Beijing, China) for providing *Ripk3^{-/-}* mice, Dr. Jianke Zhang (Thomas Jefferson University, Philadelphia, PA, USA) for providing *Fadd^{-/-}Fadd:GFP⁺*

mice and Dr. Feng Shao (National Institute of Biological Sciences, Beijing, China) for providing *Tnfr1^{-/-}* mice. We also thank Lin Qiu (Shanghai Institute of Nutrition and Health, Chinese Academy of Sciences) for technical assistance and Zhonghui Weng (Shanghai Institute of Nutrition and Health, Chinese Academy of Sciences) for mice maintained. This work was supported by grants from National Key Research and Development Program of China (2022YFA0807300), the Strategic Priority Research Program of Chinese Academy of Sciences (XDA26040306, XDB39000000), National Natural Science Foundation of China (32270803, 31970688, 82272181), Program of Shanghai Excellent Academic/Technical Research Leader (22XD1404500), Shanghai Science and Technology Commission (23141902800) and Shanghai Rising-Star Program (20QA1410800). We also thank support from Shanghai Frontiers Science Center of Cellular Homeostasis and Human Diseases, GuangCi Professorship Program of Ruijin Hospital Shanghai Jiao Tong University School of Medicine and Shanghai Municipal Science and Technology Major Project.

Author contributions

Lingxia Wang: Conceptualization; data curation; formal analysis; investigation; writing – original draft; writing – review and editing. **Xixi Zhang:** Conceptualization; formal analysis; investigation and . **Haiwei Zhang:** Formal analysis, investigation, and methodology. **Kaili Lu:** Conceptualization. **Ming Li:** Investigation and methodology. **Xiaoming Li:** Investigation and methodology. **Yangjing Ou:** Investigation and methodology. **Xiaoming Zhao:** Investigation and methodology. **Xiaoxia Wu:** Investigation and methodology. **Xuanhui Wu:** Investigation and methodology. **Jianling Liu:** Investigation and methodology. **Mingyan Xing:** Investigation and methodology. **Han Liu:** Investigation and methodology. **Yue Zhang:** Investigation and methodology. **Yongchang Tan:** Investigation and methodology. **Fang Li:** Investigation and methodology. **Xiaoxue Deng:** Formal analysis; Investigation. **Jiangshan Deng:** Formal analysis; investigation. **Xiaojie Zhang:** Formal analysis; Investigation. **Jinbao Li:** Conceptualization. **Yuwu Zhao:** Conceptualization. **Qirong Ding:** Conceptualization. **Haikun Wang:** Conceptualization. **Xiuzhe Wang:** Conceptualization; investigation; methodology; writing – review and editing. **Yan Luo:** Supervision; conceptualization; funding acquisition; writing – review and editing. **Ben Zhou:** Supervision; conceptualization; funding acquisition; resources; writing – review and editing. **Haibing Zhang:** Conceptualization; supervision; funding acquisition; writing – original draft; project administration; writing – review and editing.

Disclosure and competing interests statement

The authors declare that they have no conflict of interest.

References

- Bernal GM, Wahlstrom JS, Crawley CD, Cahill KE, Pytel P, Liang H, Kang S, Weichselbaum RR, Yamini B (2014) Loss of Nfkb1 leads to early onset aging. *Aging (Albany NY)* 6: 931–943
- Braumuller H, Wieder T, Brenner E, Assmann S, Hahn M, Alkhaled M, Schilbach K, Essmann F, Kneilling M, Griessinger C et al (2013) T-helper-1-cell cytokines drive cancer into senescence. *Nature* 494: 361–365
- Breen EC, Sehl ME, Shih R, Langfelder P, Wang R, Horvath S, Bream JH, Duggal P, Martinson J, Wolinsky SM et al (2022) Accelerated aging with HIV begins at the time of initial HIV infection. *iScience* 25: 104488
- Cai Y, Song W, Li J, Jing Y, Liang C, Zhang L, Zhang X, Zhang W, Liu B, An Y et al (2022) The landscape of aging. *Sci China Life Sci* 65: 2354–2454

- Carrasco E, Gomez de las Heras MM, Gabande-Rodriguez E, Desdin-Mico G, Francisco Aranda J, Mittelbrunn M (2021) The role of T cells in age-related diseases. *Nat Rev Immunol* 22: 97–111
- Chinnaiyan AM, O'Rourke K, Tewari M, Dixit VM (1995) FADD, a novel death domain-containing protein, interacts with the death domain of Fas and initiates apoptosis. *Cell* 81: 505–512
- Covre LP, De Maeyer RPH, Gomes DCO, Akbar AN (2020) The role of senescent T cells in immunopathology. *Aging Cell* 19: e13272
- Dannappel M, Vlantis K, Kumari S, Polykratis A, Kim C, Wachsmuth L, Eftychi C, Lin J, Corona T, Hermance N et al (2014) RIPK1 maintains epithelial homeostasis by inhibiting apoptosis and necroptosis. *Nature* 513: 90–94
- Delphine CL, Eletto D, Changxin W (2018) Biallelic RIPK1 mutations in humans cause severe immunodeficiency, arthritis, and intestinal inflammation. *Science* 361: 810–813
- Desdin-Mico G, Soto-Herederó G, Aranda JF, Oller J, Carrasco E, Gabande-Rodriguez E, Blanco EM, Alfranca A, Cusso L, Desco M et al (2020) T cells with dysfunctional mitochondria induce multimorbidity and premature senescence. *Science* 368: 1371–1376
- Dillon CP, Weinlich R, Rodriguez DA, Cripps JG, Quarato G, Gurung P, Verbist KC, Brewer TL, Llambi F, Gong Y-N et al (2014) RIPK1 blocks early postnatal lethality mediated by caspase-8 and RIPK3. *Cell* 157: 1189–1202
- Dimri GP, Lee X, Basile G, Acosta M, Scott G, Roskelley C, Medrano EE, Linskens M, Rubelj I, Pereira-Smith O (1995) A biomarker that identifies senescent human cells in culture and in aging skin in vivo. *Proc Natl Acad Sci USA* 92: 12333–12337
- Doitsh G, Galloway NL, Geng X, Yang Z, Monroe KM, Zepeda O, Hunt PW, Hatano H, Sowinski S, Munoz-Arias I et al (2014) Cell death by pyroptosis drives CD4 T-cell depletion in HIV-1 infection. *Nature* 505: 509–514
- Dowling JP, Cai Y, Bertin J, Gough PJ, Zhang J (2016) Kinase-independent function of RIP1, critical for mature T-cell survival and proliferation. *Cell Death Dis* 7: e2379
- Elyahu Y, Monsonogo A (2021) Thymus involution sets the clock of the aging T-cell landscape: implications for declined immunity and tissue repair. *Ageing Res Rev* 65: 101231
- Esteban-Cantos A, Rodriguez-Centeno J, Barruz P, Alejos B, Saiz-Medrano G, Nevado J, Martin A, Gaya F, De Miguel R, Bernardino JI et al (2021) Epigenetic age acceleration changes 2 years after antiretroviral therapy initiation in adults with HIV: a substudy of the NEAT001/ANRS143 randomised trial. *Lancet HIV* 8: e197–e205
- Fan C, Pu W, Wu X, Zhang X, He L, Zhou B, Zhang H (2016) Lack of FADD in Tie-2 expressing cells causes RIPK3-mediated embryonic lethality. *Cell Death Dis* 7: e2351
- Goldberg EL, Dixit VD (2015) Drivers of age-related inflammation and strategies for healthspan extension. *Immunol Rev* 265: 63–74
- Goronzy JJ, Weyand CM (2019) Mechanisms underlying T cell ageing. *Nat Rev Immunol* 19: 573–583
- Gross AM, Jaeger PA, Kreisberg JF, Licon K, Jepsen KL, Khosroheidari M, Morsey BM, Swindells S, Shen H, Ng CT et al (2016) Methylome-wide analysis of chronic HIV infection reveals five-year increase in biological age and epigenetic targeting of HLA. *Mol Cell* 62: 157–168
- Gupta S, Su H, Agrawal S, Gollapudi S (2018) Molecular changes associated with increased TNF-alpha-induced apoptosis in naive (T(N)) and central memory (T(CM)) CD8+ T cells in aged humans. *Immun Ageing* 15: 2
- Han S, Georgiev P, Ringel AE, Sharpe AH, Haigis MC (2023) Age-associated remodeling of T cell immunity and metabolism. *Cell Metab* 35: 36–55
- He S, Wang L, Miao L, Wang T, Du F, Zhao L, Wang X (2009) Receptor interacting protein kinase-3 determines cellular necrotic response to TNF-alpha. *Cell* 137: 1100–1111
- Huang Z, Chen B, Liu X, Li H, Xie L, Gao Y, Duan R, Li Z, Zhang J, Zheng Y et al (2021) Effects of sex and aging on the immune cell landscape as assessed by single-cell transcriptomic analysis. *Proc Natl Acad Sci USA* 118: e2023216118
- Imanishi T, Unno M, Yoneda N, Motomura Y, Mochizuki M, Sasaki T, Pasparakis M, Saito T (2023) RIPK1 blocks T cell senescence mediated by RIPK3 and caspase-8. *Sci Adv* 9: eadd6097
- Jurk D, Wilson C, Passos JF, Oakley F, Correia-Melo C, Greaves L, Saretzki G, Fox C, Lawless C, Anderson R et al (2014) Chronic inflammation induces telomere dysfunction and accelerates ageing in mice. *Nat Commun* 2: 4172
- Kubben N, Misteli T (2017) Shared molecular and cellular mechanisms of premature ageing and ageing-associated diseases. *Nat Rev Mol Cell Biol* 18: 595–609
- Li Y, Fuhrer M, Bahrami E, Socha P, Klaudel-Dreszler M, Bouzidi A, Liu Y, Lehle AS, Magg T, Hollizeck S et al (2018) Human RIPK1 deficiency causes combined immunodeficiency and inflammatory bowel diseases. *Proc Natl Acad Sci USA* 116: 970–975
- Lin J, Kumari S, Kim C, Van T-M, Wachsmuth L, Polykratis A, Pasparakis M (2016) RIPK1 counteracts ZBP1-mediated necroptosis to inhibit inflammation. *Nature* 540: 124–128
- Lopez-Otin C, Blasco MA, Partridge L, Serrano M, Kroemer G (2022) Hallmarks of aging: an expanding universe. *Cell* 186: 243–278
- Luo OJ, Lei W, Zhu G, Ren Z, Xu Y, Xiao C, Zhang H, Cai J, Luo Z, Gao L et al (2022) Multidimensional single-cell analysis of human peripheral blood reveals characteristic features of the immune system landscape in aging and frailty. *Nature Aging* 2: 348–364
- Maraskovsky E, Teepe M, Morrissey PJ, Braddy S, Miller RE, Lynch DH, Peschon JJ (1996) Impaired survival and proliferation in IL-7 receptor-deficient peripheral T cells. *J Immunol* 157: 5315–5323
- Mogilenko DA, Shpynov O, Andhey PS, Arthur L, Swain A, Esaulova E, Brioschi S, Shchukina I, Kerndl M, Bambouskova M et al (2021) Comprehensive profiling of an aging immune system reveals clonal GZMK(+) CD8(+) T cells as conserved hallmark of inflammaging. *Immunity* 54: 99–115
- Mogilenko DA, Shchukina I, Artyomov MN (2022) Immune ageing at single-cell resolution. *Nat Rev Immunol* 22: 484–498
- Newton K, Wickliffe KE, Maltzman A, Dugger DL, Strasser A, Pham VC, Lill JR, Roose-Girma M, Warming S, Solon M et al (2016) RIPK1 inhibits ZBP1-driven necroptosis during development. *Nature* 540: 129–133
- O'Donnell JA, Lehman J, Roderick JE, Martinez-Marin D, Zelic M, Doran C, Hermance N, Lyle S, Pasparakis M, Fitzgerald KA et al (2018) Dendritic cell RIPK1 maintains immune homeostasis by preventing inflammation and autoimmunity. *J Immunol* 200: 737–748
- Ofengeim D, Yuan J (2013) Regulation of RIP1 kinase signalling at the crossroads of inflammation and cell death. *Nat Rev Mol Cell Biol* 14: 727–736
- Palmer S, Albergante L, Blackburn CC, Newman TJ (2018) Thymic involution and rising disease incidence with age. *Proc Natl Acad Sci USA* 115: 1883–1888
- Rickard JA, O'Donnell JA, Evans JM, Lalaoui N, Poh AR, Rogers T, Vince JE, Lawlor KE, Ninnis RL, Anderton H et al (2014) RIPK1 regulates RIPK3-MLKL-driven systemic inflammation and emergency hematopoiesis. *Cell* 157: 1175–1188
- Roderick JE, Hermance N, Zelic M, Simmons MJ, Polykratis A, Pasparakis M, Kelliher MA (2014) Hematopoietic RIPK1 deficiency results in bone

- marrow failure caused by apoptosis and RIPK3-mediated necroptosis. *Proc Natl Acad Sci USA* 111: 14436–14441
- Spadaro O, Youm Y, Shchukina I, Ryu S, Sidorov S, Ravussin A, Nguyen K, Aladyeva E, Predeus AN, Smith SR et al (2022) Caloric restriction in humans reveals immunometabolic regulators of health span. *Science* 11: 671–677
- Sun L, Wang H, Wang Z, He S, Chen S, Liao D, Wang L, Yan J, Liu W, Lei X et al (2012) Mixed lineage kinase domain-like protein mediates necrosis signaling downstream of RIP3 kinase. *Cell* 148: 213–227
- Tan JT, Dudl E, LeRoy E, Murray R, Sprent J, Weinberg KI, Surh CD (2001) IL-7 is critical for homeostatic proliferation and survival of naive T cells. *Proc Natl Acad Sci USA* 98: 8732–8737
- Thomas R, Wang WK, Su DM (2020) Contributions of age-related thymic involution to immunosenescence and inflammaging. *Immun Ageing* 17: 2
- Uchiyama Y, Kim CA, Pastorino AC, Ceroni J, Lima PP, de Barros DM, Honjo RS, Bertola D, Hamanaka K, Fujita A et al (2019) Primary immunodeficiency with chronic enteropathy and developmental delay in a boy arising from a novel homozygous RIPK1 variant. *J Hum Genet* 64: 955–960
- Webb LV, Barbarulo A, Huysentruyt J, Vanden Berghe T, Takahashi N, Ley S, Vandenabeele P, Seddon B (2019) Survival of single positive thymocytes depends upon developmental control of RIPK1 kinase signaling by the IKK complex independent of NF-kappaB. *Immunity* 50: 348–361
- Xu D, Jin T, Zhu H, Chen H, Ofengeim D, Zou C, Mifflin L, Pan L, Amin P, Li W et al (2018) TBK1 suppresses RIPK1-driven apoptosis and inflammation during development and in aging. *Cell* 174: 1477–1491
- Yousefzadeh MJ, Flores RR, Zhu Y, Schmiechen ZC, Brooks RW, Trussoni CE, Cui Y, Angelini L, Lee KA, McGowan SJ et al (2021) An aged immune system drives senescence and ageing of solid organs. *Nature* 594: 100–105
- Zhang Y, Rosenberg S, Wang H, Imtiyaz HZ, Hou YJ, Zhang J (2005) Conditional Fas-associated death domain protein (FADD): GFP knockout mice reveal FADD is dispensable in thymic development but essential in peripheral T cell homeostasis. *J Immunol* 175: 3033–3044
- Zhang X, Fan C, Zhang H, Zhao Q, Liu Y, Xu C, Xie Q, Wu X, Yu X, Zhang J et al (2016) MLKL and FADD are critical for suppressing progressive lymphoproliferative disease and activating the NLRP3 inflammasome. *Cell Rep* 16: 3247–3259
- Zhang X, Zhang H, Xu C, Li X, Li M, Wu X, Pu W, Zhou B, Wang H, Li D et al (2019) Ubiquitination of RIPK1 suppresses programmed cell death by regulating RIPK1 kinase activation during embryogenesis. *Nat Commun* 10: 4158
- Zhang H, Weyand CM, Goronzy JJ (2021) Hallmarks of the aging T-cell system. *FEBS J* 288: 7123–7142
- Zheng Y, Liu X, Le W, Xie L, Li H, Wen W, Wang S, Ma S, Huang Z, Ye J et al (2020) A human circulating immune cell landscape in aging and COVID-19. *Protein Cell* 11: 740–770